Closed-Loop Control of Active Sensing Movements Regulates Sensory Slip

Debojyoti Biswas,[1] Luke A. Arend,[1] Sarah A. Stamper,[1] Balázs P. Vágvölgyi,[1] Eric S. Fortune,[2] and Noah J. Cowan[1,*]

[1] *Johns Hopkins University, Baltimore, MD 21218*

[2] *New Jersey Institute of Technology, Newark, NJ 07102*

SUMMARY

Active sensing is the production of motor signals for sensing [1–5]. The most common form of active sensing, found across animal taxa and behaviors, involves the generation of movements—e.g. whisking [6–8], touch [9, 10], sniffing [11, 12], and eye movements [13]—that shape spatiotemporal patterns of feedback. Despite the fact that active-sensing movements profoundly affect the information carried by sensory feedback pathways [14–16], how such movements are regulated remains poorly understood. To investigate the control of active-sensing, we created an augmented reality apparatus for freely swimming weakly electric fish, *Eigenmannia virescens*. This system modulates the gain of reafferent feedback by adjusting the position of a refuge based on real time videographic measurements of fish position. We discovered that fish robustly regulate sensory slip via closed-loop control of active-sensing movements. Specifically, as fish performed the task of maintaining position inside the refuge [17–22], they dramatically up- or down-regulated fore-aft active sensing movements in relation to a 4-fold change of experimentally modulated reafferent gain. These changes in swimming movements served to maintain a constant magnitude of sensory slip. The magnitude of sensory slip depended on the presence or absence of visual cues, but in each condition the respective magnitude was maintained across reafferent gains. These results indicate that fish use two control loops: an "inner loop" that controls the acquisition of information by regulating sensory slip, and an "outer loop" that maintains position in the refuge, a control topology that may be ubiquitous in animals [23, 24].

RESULTS

Active sensing is modulated by reafferent gain

As the fish maintains its position within a refuge, it also produces small fore-aft body movements [15]. These small movements create a dynamic difference between the position of the fish and the refuge, i.e. a *sensory slip* analogous to retinal slip [24, 25], albeit mediated by the propagation of electricity in water [4]. Active swimming movements in these fish likely prevent perceptual fading and shape spatiotemporal patterns of sensory feedback [15] serving a similar role as small eye movements in the visual system [16, 26].

A key question we address in this paper is whether the active movements depend on the electrosensory feedback they produce (i.e., are the active movements under closed-loop control) or are active movements independent of this feedback (i.e., open loop). To determine the functional relationships between the production of active movements and the resulting reafferent feedback, we designed an experimental apparatus in which the animal performs refuge tracking inside an "augmented reality" system. Custom software tracks the position of the fish in real time and uses this measurement to adjust the position of the refuge with a low-latency controller (see Fig. 1 A,B and *STAR Methods*). The movement of the refuge is determined by the movement of the fish based on an experimentally defined gain, γ (see Fig. 1 C).

The critical feature of this augmented reality system is that reafferent feedback from self movement can be experimentally modulated. In the veridical condition, the fish experiences an equal-but-opposite sensory slip to its own movement (reafferent gain of -1). When the refuge, $r(t)$, is moved in relation to the fish, $x(t)$, via an experimentally applied gain, γ, the refuge motion is given by $r(t) = \gamma x(t)$. Thus, the sensory slip, or "error", is given as follows:

$$\begin{aligned} e(t) &= r(t) - x(t) \\ &= \gamma x(t) - x(t) \\ &= \underbrace{(\gamma - 1)}_{\text{Reafferent gain}} \quad x(t) \end{aligned} \tag{1}$$

For example, when the experimental gain is set to $\gamma = 0.22$, the ovement of the refuge follows the position of the fish but at a smaller amplitude, thereby reducing the sensory slip (reafferent gain of -0.78). When the experimental gain is $\gamma = -1$ the refuge moves as fast as the fish, but in the opposite direction (reafferent gain of -2; see Fig. 1 D). See supplementary movies. When $\gamma = 0$, the fish's reafferent feedback is -1, the natural condition used in all prior studies [17–20, 22].

We performed two categories of experiments: **augmented feedback experiments** in which the animals perform station-keeping in the apparatus described above, and **playback experiments** ($\gamma = 0$, natural reafferent gain of -1) in which we replayed trajectories of the refuge (see Fig. 1 E,F and *STAR Methods*). These refuge trajectories were recorded during previous closed-loop trials. The movement of the refuge was identical across open- and closed-loop trials making the only difference between these trials the reafferent gain experienced by the fish. Thus, the sole experimental variable is whether or not a closed-loop coupling exists between the movements of the fish and those of the refuge. This manipulation isolates the effects of enhancing or suppressing sensory feedback from the details of the refuge trajectory, since the latter is identical across open- and closed-loop experiment.

As a measure of animal's movement and the resulting sensory slip, we calculated the root-mean-squared (RMS) of both signals, a common measure of signal magnitude:

$$\begin{aligned} x_{\text{rms}} &= \sqrt{\frac{1}{T}\int_0^T x(t)^2 dt} \quad \text{active movement} \\ e_{\text{rms}} &= \sqrt{\frac{1}{T}\int_0^T e(t)^2 dt} \quad \text{sensory slip} \end{aligned} \tag{2}$$

If active movements did not rely on feedback control, these movements should be similar across open- and closed-loop tri-

* Correspondence: Noah J. Cowan, E-mail: ncowan@jhu.edu

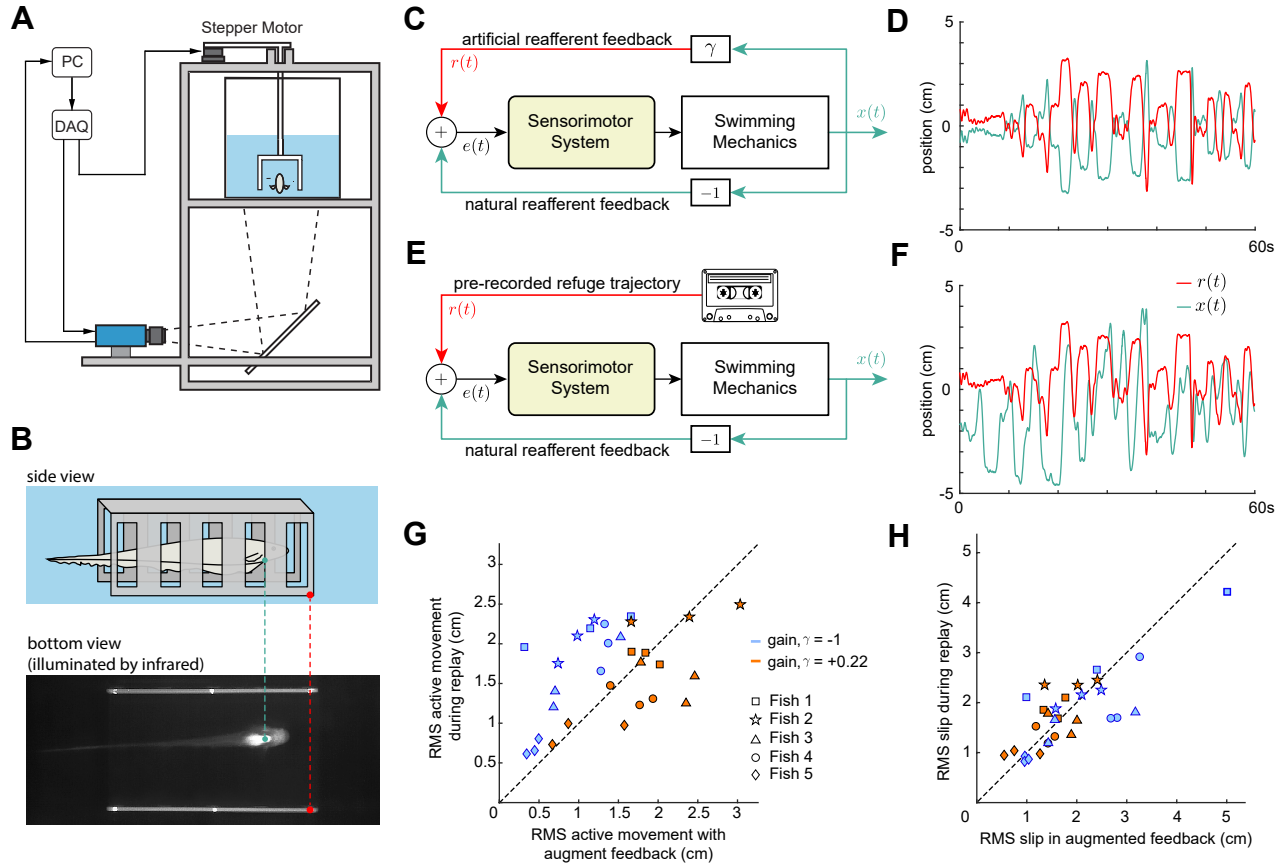

FIG. 1. Categorical differences between augmented feedback experiments and playback experiments. (A) Schematic showing a front view *E. virescens* inside a moving refuge. The refuge is actuated by a stepper motor, controlled by a computer that processes video images streamed from a camera in real time. The camera is positioned to observe the fish and refuge from below via a mirror. (B) Side view (schematic) and bottom view (image) of a fish inside the refuge. The fish has a ventral bright patch (aqua dot) in the infrared-illuminated video that can be tracked as the fish swims inside the refuge (red dot). (C) Augmented feedback experiment. The fish position, $x(t)$, is multiplied by the experimental gain γ to control the refuge position, $r(t)$. (D) Sample data for an augmented feedback experiment with gain $\gamma = -1$; aqua is the position of the fish and red the refuge. (E) Playback experiment. A pre-recorded refuge trajectory from the augmented feedback experiment is used as refuge motion $r(t)$. (F) Sample data from a playback experiment in which the refuge trajectory from (D) was replayed. Fish trajectories in (D) and (F) are markedly different despite identical refuge trajectories. (G) The root-mean-square (RMS) of active movements differed between augmented feedback and playback conditions, and depended on the gain γ. Each marker shape represents a different fish, each point is the mean of 5 trials. Blue indicates a gain of $\gamma = -1$ and orange $\gamma = +0.22$. The dashed line corresponds to the null hypothesis of equal RMS active movement for both gains. (H) Sensory slip between experimental conditions was maintained, irrespective of gain. Colors and marker shapes as in (G).

als. However, we observed less movement in closed-loop trials with a negative gain (enhanced reafference) than during the corresponding open-loop replay trials (see Fig. 1 G). Conversely, with a positive gain (attenuated reafference) gain, we observed more movement in closed-loop trials than in the corresponding open-loop trials. The ratio of open-loop to closed-loop RMS active movements were significantly different depending on the experimental gain (for $\gamma = -1$: ratio = 2.033, SEM = 0.31; for $\gamma = +0.22$: ratio = 0.912, SEM = 0.06, across fish; paired t-test: $t(4) = 4.0660$, $p = 0.015$, see *STAR Methods* for details).

In contrast, we observed no significant difference between RMS sensory slip in closed-loop and open-loop replay trials (see Fig. 1 H, for $\gamma = -1$: ratio = 0.963, SEM = 0.11; for $\gamma = +0.22$: ratio = 1.147, SEM = 0.08, across fish; paired t-test: $t(4) = 1.8596$, $p = 0.1365$).

Taken together, these results demonstrate that reafferent feedback is used to control movements for active sensing. The question remains, what is the goal of this feedback control system?

Fish regulate sensory slip across reafferent gain

Our hypothesis is that fish maintain sensory slip, i.e. fish will swim more or less as needed to generate a constant level of RMS positional slip between the fish and the refuge. To examine this hypothesis, we experimentally varied the reafferent gain, $\gamma - 1$, over the range -2 to -0.5 and measured the resulting RMS sensory slip. Previous work has shown that active sensing movements differ dramatically depending on lighting: in the dark, the movements are much larger than in the light [15]. Therefore, we investigated a second hypothesis that the set point for this regulation of sensory slip depends on the lighting condition.

From Eqn. (1), the sensory slip experienced by the fish in the augmented reality apparatus with augmented gain γ is given as follows:

$$e(t) = (\gamma - 1)x(t) \tag{3}$$

Given this relation, a straight-forward calculation shows that

the root-mean-square of the slip signal, e_{rms}, and the fish position, x_{rms}, for each gain and lighting condition must be related by a constant factor:

$$e_{\mathrm{rms}} = |\gamma - 1| x_{\mathrm{rms}} \tag{4}$$

We selected gains that ensure $1 - \gamma > 0$, and hence:

$$x_{\mathrm{rms}} = \frac{1}{1-\gamma} e_{\mathrm{rms}} \tag{5}$$

Defining $\beta = (1-\gamma)^{-1}$ simplifies this equation:

$$x_{\mathrm{rms}} = e_{\mathrm{rms}} \times \beta \tag{6}$$

Therefore, if the fish were to maintain constant RMS slip e_{rms} (invariant to the reafferent gain), then x_{rms} would be a linear function of the transformed gain β, with zero intercept and with slope given by the RMS slip, e_{rms}. More generally, if the fish were to modulate its swimming behavior to regulate RMS slip, we would expect the fish movement to increase as a function of increasing β:

$$x_{\mathrm{rms}} = f(\beta) \quad \text{(robust slip hypothesis)}$$

where $f(\cdot)$ is a monotonically increasing function.

In the null hypothesis, the active movements do not depend on the immediate feedback they create (open-loop strategy), thus we would expect the swimming motions to be invariant to applied gain:

$$x_{\mathrm{rms}} = \text{const.} \quad \text{(null hypothesis)}$$

To test these hypotheses, we selected values for β to be uniformly spaced between 0.5 and 2, corresponding to γ being nonuniformly spaced between -1 and 0.5. We found that RMS movement increased as a function of β for each individual animal (Fig. 2A,C; Mann-Kendall test, $p < 0.001$ for each of $N = 6$ fish for each lighting condition). Fitting a line through the origin $x_{\mathrm{rms}} = \text{const} \times \beta$ explained 88% of the variance across fish in the light and 65% of the variance in the dark (see Table S1; Recall that R^2 is by definition zero for the null hypothesis since the constant is simply the mean.) A quadratic curve improved the fit for the dark trials (adjusted $R^2 = 0.88$; polynomials above order 2 did not improve adjusted R^2; Table S1). The monotonically increasing RMS movements served to generate nearly constant RMS slip (Fig. 2B,D). The deviation from the linear trend at high positive gains in the dark may be a consequence of a motor/energetic trade-off: the highest values of gain would require 2× more RMS movements to maintain constant RMS slip. This deviation caused the RMS slip to decrease slightly over the full range of gains tested, as shown.

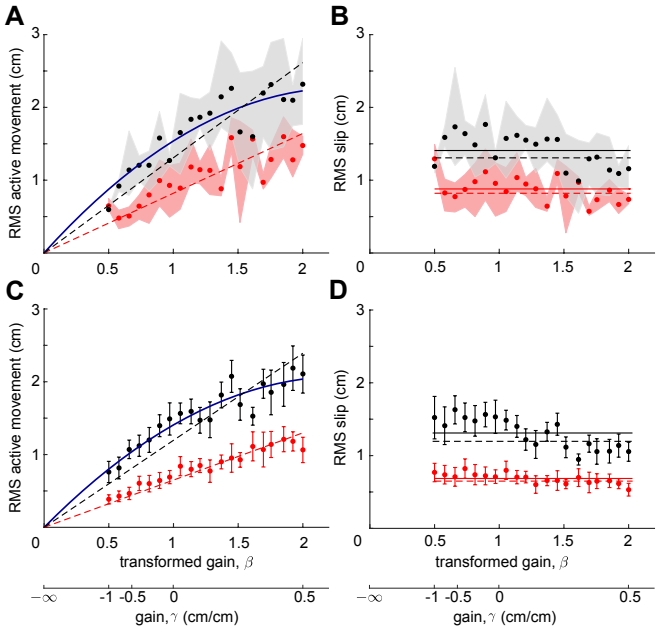

FIG. 2. Sensory slip is maintained across reafferent gains. (A) Representative data from one fish showing that RMS movements increased as a function of transformed gain, β. Each marker represents the mean across three replicates (black: 'lights-off', red: 'lights-on') at different gain values. Shaded regions denote the maximum and minimum experimental values at each gain. Dashed lines correspond to the best linear fits (through the origin, see text). A quadratic (blue, solid) improved the fit for the 'lights-off' trials. (B) For the same fish, RMS slip was approximately constant across β. Format as in (A). The dashed horizontal lines correspond to the average sensory slip predicted from the RMS active movement in (A). The solid lines correspond to the best fit horizontal lines. (C,D) Combined data for all individuals ($N = 6$) with mean ± SEM indicated.

To increase active sensing, fish swim farther, not faster

How do fish regulate RMS slip across gains? The most obvious means by which to increase the RMS of a signal would be to increase the amplitude of active sensing movements. This strategy would increase the velocity at each instant by the same factor, and would therefore cause the RMS velocity to follow an identical monotonic trend as position, holding RMS velocity slip constant. We examined if fish use this strategy—i.e. swimming faster—to maintain sensory slip. Instead, the RMS velocity changed remarkably little over the same range in gains. Fitting a constant to the RMS velocity data predicts a hyperbolically decreasing RMS velocity slip, which indeed is a good approximation ($R^2 = 0.88$ in the light, $R^2 = 0.90$ in the dark). See Fig. 3. This result implies that fish did not simply increase or decrease their velocity in order to maintain the magnitude of RMS sensory slip.

Next we analyzed the power spectral density (PSD) of active movement and sensory slip. We observed that peaks in each fish's active movement (see Fig. 3 E,F) occur at low frequencies (< 0.1 Hz). The amplitude of these peaks increase as β was increased in both light and dark conditions (see Fig. S1, Table S2). In contrast, we did not observe changes in power at higher frequencies as we changed β. This measure shows that fish are not relying on changes in rapid fore-aft movements, but rather use low-frequency fore-aft movements to compensate for changes in feedback gain.

How did the gain-dependent changes in the PSD of active movements affect sensory slip? The PSD of sensory slip is highest at low frequency (Fig. 3G,H, Fig. S1). The fish increased the low-frequency power of active movements as a function of β (Spearman's rank correlation coefficient, $\rho_s \geq 0.71$, $N = 6$), thereby maintaining the low-frequency power of slip. Further, the fish did not significantly alter high-frequency power of active movements as a function of β, and therefore the power of sensory slip at high frequencies

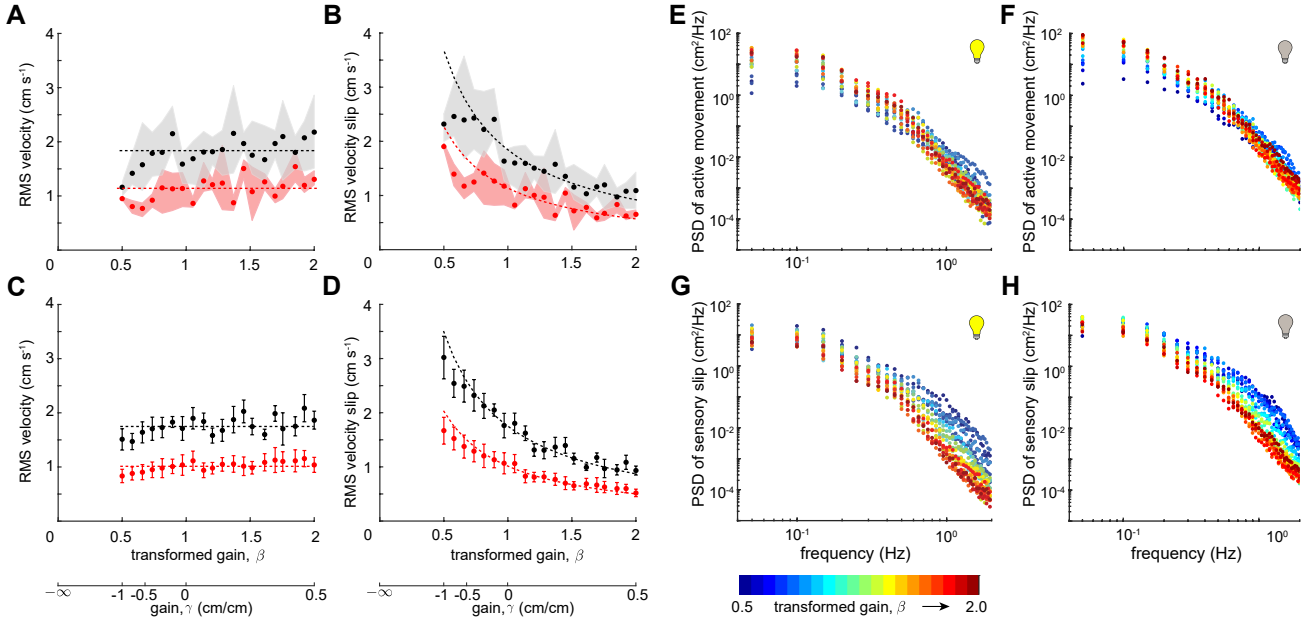

FIG. 3. Fish do not simply increase velocity to maintain robust slip. (A) Representative data showing RMS velocity as a function of transformed gain, β. Each marker represents the mean across three trials and the shaded regions indicate the maximum and minimum of these trials (black: 'lights-off', red: 'lights-on'). (B) The RMS velocity slip for the same fish, again averaged across three replicates. Same format as in (A). (C,D) Combined data for all individuals ($N = 6$) with mean ± SEM indicated. The dashed lines in (A,C) are the constant fits to the data and in (B,D) the corresponding hyperbolic predictions. (E,F) Representative data from one fish showing PSD of fish movements in light (E) and dark (F). For each gain (indicated by color) the PSD was averaged across three trials. At low frequencies but not high frequencies, increasing gain β is correlated with increased power (nearly 50 fold change from blue to red dots). (G,H) Representative data from the same fish showing the PSD of sensory slip (fish relative to refuge) in light (G) and in dark (H). At low frequencies, the power spectrum of slip is largely independent of gain β (less than 10 fold difference and colors overlapping). At high frequencies slip is highly gain dependent (blue dots nearly 100 fold above red).

decreased with increased gain β ($\rho_s \leq -0.82$, $N = 6$). To quantify the transition from low to high frequency, we measured the -10 dB cut off (0.1 amplitude crossover) frequency and found that the cut-off frequency decreased as a function of β (see Fig. S1, Table S2).

To further understand the mechanism that fish used to modulate the low-frequency power of active movements as a function of reafferent gain, we segmented the swimming trajectories into "epochs"—continuous bouts of swimming in a single direction (see *STAR Methods* and Fig. S2). We examined how these epochs changed as a function of reafferent gain and lighting. There was a significant increase in the mean epoch duration in light in compared to dark ($p_{\text{one-tail}} < 0.05$, for 5 out of 6 individuals, Mann-Whitney-Wilcoxon test). We also observed that both the epoch distance (active movement between successive direction reversals) and epoch duration (time between successive direction reversals) increase significantly with refuge gain ($N = 6$, see Table S3). Thus, the overall mechanism for increasing RMS position (regulating RMS slip) is to swim farther for each active swimming epoch by increasing its duration rather than scaling up the overall swimming speed.

Experimentally induced closed-loop filtering does not explain changes in active sensing

As a final control, we considered the possibility that the apparent change in active sensing could be explained solely by the change in closed-loop dynamics caused by our experimentally altered reafferent gain. In other words, what if the fish's strategy were strictly open loop, but the resulting RMS fish motions were changing as an artifact of the (experimentally modulated) closed-loop dynamics?

To investigate this possible confound, consider the closed-loop diagram in Fig. 4 A. Here, we model active sensing as resulting from an active probe signal, $a(t)$, generated by the nervous system. We assume that the fish's task controller and swimming mechanics (task plant) are as described in [17, 27]. The null hypothesis of open-loop active signal generation would imply that the power spectral density of the probe signal $a(t)$ should be invariant to the experimentally augmented feedback gain. In contrast, changes in the PSD of $a(t)$ as a function of the feedback gain must arise from the feedback control in the animal. We illustrate these alternatives in Fig. 4 A: the active probe signal $a(t)$ emerges from an "Active Signal Generator". If the Active Signal Generator is operating in closed-loop, then it modifies the power spectrum of $a(t)$ depending on feedback (dashed-line marked with "?" in Fig. 4 A).

For each gain, we estimated the PSD for $a(t)$ using the following relationship:

$$\text{PSD}\{a(t)\} = \frac{1}{|G_\gamma(j\omega)|^2}\text{PSD}\{x(t)\}$$

where G_γ is the transfer function relating $a(t)$ to $x(t)$ (see *STAR Methods*). We observed a substantial gain-dependent shift (two orders of magnitude) in the power spectrum of $a(t)$ (see Fig. 4 B,C, Table S4), supporting the hypothesis that fish dynamically regulate their active movements in relation

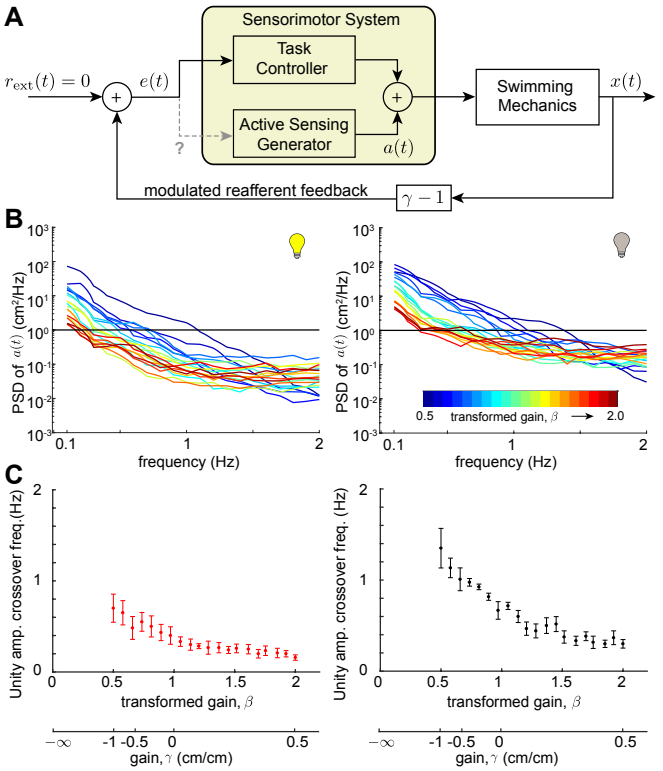

FIG. 4. Fish dynamically modulate active sensing. (A) Schematic of closed-loop experimental setup with active probe signal, $a(t)$. External input signal, $r_{\text{ext}}(t)$ is zero in the present study. (B) Representative estimate of power spectra of $a(t)$ for movements of an individual fish during 'lights-on' trials (left) and 'lights-off' trials (right). The solid black line corresponds to amplitude 1 cm^2/Hz. We found that $a(t)$ depends on β. (C) Combined data of unity-power cross over frequency of $a(t)$ for all individuals ($N = 6$) with mean ± SEM under different lighting conditions (red: 'lights-on', black: 'lights-off').

to ongoing sensory feedback. These data reject the hypothesis that the closed-loop filtering properties of our augmented reality system leads to the the observed changes in active sensing behavior.

DISCUSSION

We developed an augmented reality system to investigate how active sensing movements in *Eigenmannia virescens* are controlled. We found that the magnitude of these movements depends on the gain of reafferent sensory feedback, indicating that active sensing movements are under feedback control. The experiments also revealed that the fish maintain nearly constant-magnitude sensory slip across changes in reafferent gain, showing that a goal of the feedback control system is the maintenance of RMS slip. These findings suggest that there are separate control systems for active sensing and goal-directed behavior: an "inner" control loop manages the flow of sensory information for an "outer" control loop that uses this information to achieve task-level behavior. This control topology is likely used for active sensing across modalities and species.

Fish made adjustments in active sensing movements to maintain sensory slip across manipulations of the gain of reafferent feedback both in the presence and absence of salient visual cues. The magnitude of sensory slip in the light was categorically less than in the dark, consistent with prior work [15]. In contrast, the relations between adjustments in conductivity—which affects electrosensory feedback but not vision or other modalities—and the magnitude of fore-aft movements [15] demonstrates that these movements are used almost exclusively for active sensing in the electrosensory domain. The lower set point for the magnitude of active sensing movements in the light reflects a reliance on visual cues over electrosensory cues for tracking the position of the refuge. Indeed, fish dynamically lower their gain to electrosensory information for refuge tracking when salient visual cues are available [21].

Recent work has shown that ON and OFF cells in the hindbrain can give rise to bursts of activity that encode reversals in the direction of movement of looming/receding stimuli [28]. These sorts of bursts may also contribute to the detection of reversals of longitudinal movement [29]. In the midbrain, neurons encode velocity of longitudinal moving objects, so-called direction-selective neurons [30–34]; midbrain neurons are sensitive to specific ranges of temporal frequencies [35–37] and velocities of motion [34, 38]. How do these computations relate to the control of active sensing? The maintainance of RMS slip across feedback gains was achieved by increasing the durations of epochs of sensory slip, while the numbers of reversals in the direction of sensory slip were not maintained across gains. This suggests that the control of active sensing is not tuned to regulate the stimulation of reversal-sensitive neurons. Instead, the changes in epoch duration but not the velocity of sensory slip suggest that the movements may be tuned to the temporal filtering properties of direction selective neurons.

Critically, neural circuits for active sensing must be modulated in relation to task. The active sensing movements are not conserved across electrosensory behaviors; for example the impulsive nature of prey capture movements [39] are categorically different than refuge tracking. Recent findings suggest potential substrates for task-dependent modulation of sensory processing via descending feedback pathways. For example, rather than relying solely on bottom-up computations, encoding of looming/receding objects is mediated by descending feedback from the midbrain [28]. Similary, feedback rather than feed-forward information processing is involved in extracting electrosensory envelope information (a correlate of distance) [40].

This structure for closed-loop control of active sensing–an inner loop for feedback control of active sensing and an outer loop for feedback control of task-directed movements–likely occurs across modalities and species. For example, in rats the timing of whisker protraction is locked to contact events, suggesting that whisking movements are under feedback control [23]. In humans, saccadic eye movements are triggered by low retinal slip [24], also suggesting that they are under feedback control.

This feedback control topology can be applied to engineered systems. The generation of active sensing movements can ensure a system property known as *observability* [41–43]—i.e. sufficient sensory information to enable estimation of the system state (i.e. position and velocity)—upon which the task-level controller can act.

Closed-loop experimental approaches [6, 44] are crucial for disentangling complex interactions between sensing and control [45–47]. This is highlighted by the open-loop replay exper-

iments: fish produced different output behavior based solely on whether the stimulus emerged from a closed-loop interaction or was replayed in open loop. This categorical shift in responses in open- and closed-loop may be a widespread feature of animal behavior [48, 49].

ACKNOWLEDGMENTS

Thanks to Kyle Yoshida and Ismail Uyanik for helping with data collection. This material is based upon work supported by a Complex Systems Scholar Award to NJC from the James McDonnell Foundation under Grant No. 112836, a Collaborative National Science Foundation Award to NJC and ESF under Grant Nos. 1557895 and 1557858, an NSF REU to LAA under Grant No. 1460674, and a Johns Hopkins Electrical Engineering graduate fellowship to DB.

AUTHOR CONTRIBUTIONS

DB and LAA collected and analyzed the data and prepared a draft of the manuscript. BPV designed and built the novel experimental apparatus. SAS and ESF contributed to the conception of the experiment and interpretation of the results. SAS collected preliminary data and performed statistical analysis. NJC led the experimental design and interpretation of results. All authors participated in revisions to the manuscript, and have approved the final version.

DECLARATION OF INTERESTS

The authors declare no competing interests.

[1] R. Bajcsy, Proceedings of the IEEE **76**, 996 (1988).
[2] W. W. Au and J. A. Simmons, Phys Today **60**, 40 (2007).
[3] C. Assad, B. Rasnow, and P. K. Stoddard, J Exp Biol **202**, 1185 (1999).
[4] D. Babineau, J. E. Lewis, and A. Longtin, PLoS Comp Biol **3**, e38 (2007).
[5] G. von der Emde, J Comp Physiol A **192**, 601 (2006).
[6] D. H. O'connor, S. A. Hires, Z. V. Guo, N. Li, J. Yu, Q.-Q. Sun, D. Huber, and K. Svoboda, Nat Neurosci **16**, 958 (2013).
[7] R. A. Grant, B. Mitchinson, C. W. Fox, and T. J. Prescott, J Neurophysiol **101**, 862 (2009).
[8] M. J. Hartmann, Autonomous Robots **11**, 249 (2001).
[9] T. J. Prescott, M. E. Diamond, and A. M. Wing, Philos Trans R Soc B **366**, 2989 (2011).
[10] A. Saig, G. Gordon, E. Assa, A. Arieli, and E. Ahissar, J Neurosci **32**, 14022 (2012).
[11] S. Ranade, B. Hangya, and A. Kepecs, J Neurosci **33**, 8250 (2013).
[12] M. Wachowiak, Neuron **71**, 962 (2011).
[13] E. Ahissar and A. Arieli, Front Comp Neurosci **6** (2012).
[14] S. C.-H. Yang, D. M. Wolpert, and M. Lengyel, Curr Opin Behav Sci **11**, 100 (2016).
[15] S. A. Stamper, E. Roth, N. J. Cowan, and E. S. Fortune, J Exp Biol **215**, 1567 (2012).
[16] N. Mostofi, M. Boi, and M. Rucci, Vision Res **118**, 60 (2016).
[17] N. J. Cowan and E. S. Fortune, J Neurosci **27**, 1123 (2007).
[18] E. Roth, K. Zhuang, S. A. Stamper, E. S. Fortune, and N. J. Cowan, J Exp Biol **214**, 1170 (2011).
[19] G. J. Rose and J. G. Canfield, J Comp Physiol A **173**, 698 (1993).
[20] G. J. Rose and J. G. Canfield, J Comp Physiol A **171**, 791 (1993).
[21] E. E. Sutton, A. Demir, S. A. Stamper, E. S. Fortune, and N. J. Cowan, J R Soc Interface **13**, 20160057 (2016).
[22] N. J. Cowan, M. M. Ankarali, J. P. Dyhr, M. S. Madhav, E. Roth, S. Sefati, S. Sponberg, S. A. Stamper, E. S. Fortune, and T. L. Daniel, Integr Comp Biol **54**, 223 (2014).
[23] B. Mitchinson, C. J. Martin, R. A. Grant, and T. J. Prescott, Proc R Soc Lond [Biol] **274**, 1035 (2007).
[24] R. Engbert and K. Mergenthaler, Proc Nat Acad Sci **103**, 7192 (2006).
[25] R. V. Abadi and R. Worfolk, Vision Research **29**, 195 (1989).
[26] L. A. Riggs, F. Ratliff, J. C. Cornsweet, and T. N. Cornsweet, J Opt Soc Am **43**, 495 (1953).
[27] S. Sefati, I. D. Neveln, E. Roth, T. R. Mitchell, J. B. Snyder, M. A. MacIver, E. S. Fortune, and N. J. Cowan, Proc Nat Acad Sci **110**, 18798 (2013).
[28] S. E. Clarke and L. Maler, Current Biology **27**, 1356 (2017).
[29] S. E. Clarke, A. Longtin, and L. Maler, J. Neurosci. **34**, 5583 (2014).
[30] J. Ramcharitar, E. Tan, and E. Fortune, J Neurophysiol **96**, 2319 (2006).
[31] S. G. Carver, E. Roth, N. J. Cowan, and E. S. Fortune, PLoS Comp Biol **4** (2008), pMC2242823.
[32] M. Chacron, N. Toporikova, and E. Fortune, J Neurophysiol **102**, 3270 (2009).
[33] M. Chacron and E. Fortune, J Neurophysiol **104**, 449 (2010).
[34] N. Khosravi-Hashemi, E. S. Fortune, and M. J. Chacron, J Neurophysiol **106**, 1954 (2011).
[35] E. S. Fortune and G. J. Rose, Trends Neurosci **24**, 381 (2001).
[36] G. J. Rose and E. S. Fortune, J Exp Biol **202**, 1281 (1999).
[37] E. S. Fortune and G. J. Rose, J Neurosci **17**, 3815 (1997).
[38] J. Ramcharitar, E. Tan, and E. Fortune, J Comp Physiol A **191**, 865 (2005).
[39] M. E. Nelson and M. A. Maciver, J Exp Biol **202**, 1195 (1999).
[40] M. G. Metzen, C. G. Huang, and M. J. Chacron, PLoS Biol **16**, e2005239 (2018).
[41] A. Kunapareddy and N. J. Cowan, in *Proc Amer Control Conf* (Milwaukee, WI, USA, 2018) submitted.
[42] B. T. Hinson, M. K. Binder, and K. A. Morgansen, in *Proc Amer Control Conf* (IEEE, 2013) pp. 1392–1399.
[43] S. Cedervall and X. Hu, IEEE Trans Autom Control **52**, 1325 (2007).
[44] F. Engert, Front Neural Circuits **6**, 125 (2013).
[45] E. Roth, S. Sponberg, and N. J. Cowan, Curr Opin Neurobiol **25**, 54 (2014).
[46] E. D. Tytell, C.-Y. Hsu, and L. J. Fauci, Zoology **117**, 48 (2014).
[47] M. S. Madhav, S. A. Stamper, E. S. Fortune, and N. J. Cowan, J Exp Biol **216**, 4272 (2013).
[48] C. Kim, T. Ruberto, P. Phamduy, and M. Porfiri, Sci Rep **8**, 657 (2018).
[49] E. Roth, M. B. Reiser, M. H. Dickinson, and N. J. Cowan, in *Proc IEEE Int Conf on Decision Control* (IEEE, 2012) pp. 3721–3726.

STAR⋆METHODS

CONTACT FOR REAGENT AND RESOURCE SHARING

Further information and requests for data/protocols should be directed to and will be fulfilled by the Lead Contact, Noah J. Cowan (ncowan@jhu.edu).

EXPERIMENTAL MODEL AND SUBJECT DETAILS

Subjects

Adult *Eigenmannia virescens* (10-15 cm in length) were obtained from commercial vendors and housed according to published guidelines [1]. The experimental tanks were maintained with a water temperature of $\sim$27 °C and conductivity in the range of 150-250 µS cm^{-1}. All experimental procedures were approved by the Johns Hopkins Animal Care and Use Committee and followed guidelines established by the National Research Council and the Society for Neuroscience.

METHOD DETAILS

Experimental apparatus and procedure

The experimental apparatus was similar to that described in previous studies [2, 3]. The test environment was a 17 gallon rectangular glass aquarium. The refuge was machined from a 111 mm (111.66 ± 0.23) segment of 46.64×50.65 ($46.64 \pm 0.33 \times 50.65 \pm 0.10$) mm gray rectangular PVC tubing. The bottom face of the tube was removed and a series of five rectangular windows (6 mm in width and spaced 19 mm apart) were machined into each side to provide visual and electrosensory cues. The refuge was suspended less than 0.5 cm above the floor of the tank by an acrylic mount attached to a linear stepper motor (STS-0620-R, HW W Technologies, Inc., Valencia, CA, USA).
Prior to trials, an individual fish was transferred to the testing tank and allowed to acclimate for 4-24 hr. During trials, the position of the fish inside the refuge was recorded using a video camera (pco.1200, PCO AG, Kelheim, Germany). Video was captured at 25 frames per second and the position of the fish was tracked in real time using custom vision software programmed in LabView (National Instruments, Austin, TX, USA). Altogether, this allowed an experimental paradigm where the refuge could be moved either with a gain directly proportional to the movements of the fish (experimentally closed loop) or with a specified trajectory (experimentally open loop).
The LabView-based video tracking algorithm employed template matching to determine the position of the fish in the video frames. For each fish, a custom image template was generated based on its appearance. Camera images were calibrated to determine the physical size of the area covered by each pixel in the plane that the fish swam so that we could estimate the physical location of the fish within the refuge. Given the requirement of low latency, we implemented an FPGA-based stepper motor controller in LabView that was directly controlled by the image-processing PC, sending it target positions as soon as the physical position of the fish was determined by the image-processing software. The stepper motor controller generated the fastest possible smooth trajectory to the target position and sent the corresponding pulse train to the motor driver. We controlled the camera frame rate using the same FPGA hardware along with the manual shutter feature of the camera. The capture frame rate was fixed at 25 frames per second and the image-capture-to-motor-control latency was less than one video frame time (< 40 ms).

Closed-loop and open-loop experiments

Closed-loop experiments were 70 s in duration comprising three phases: Initiation (5 s duration), Cross-Fade (5 s) and Test (60 s duration). All of the data and analysis reported in these experiments are from the Test Phase. See Fig. 1 A,B.

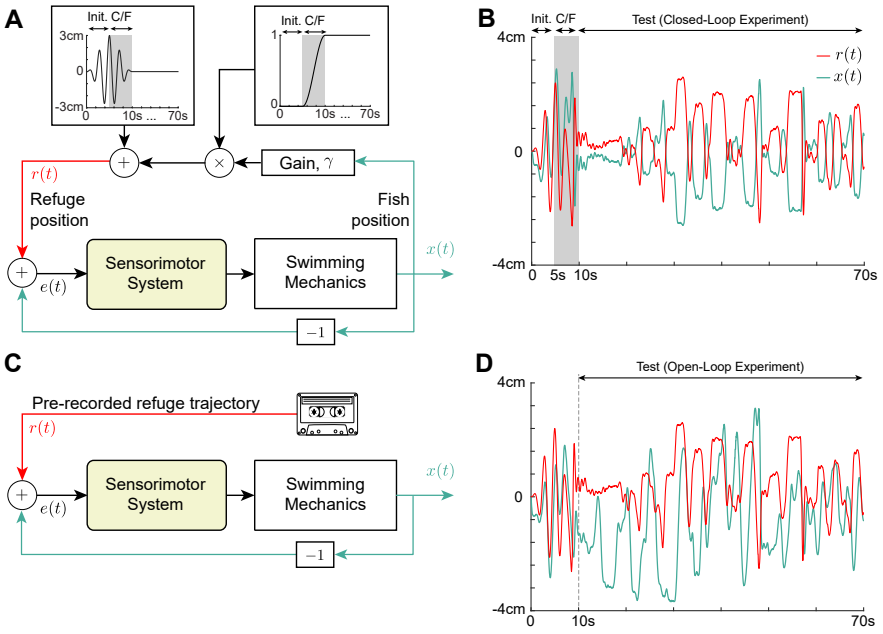

FIG. 1. Implementation of different experimental phases and sample trajectories. (A) Closed-loop experiment. The fish position, $x(t)$, is transformed to yield the intended refuge position, $r(t)$, via multiplications with gain constant γ and a 'cross-fade' signal before being added to a smooth sinusoidal onset signal (see text for details). (B) Sample data for a closed-loop experiment with gain $\gamma = -1$. First 5 seconds of the trial are Initiation Phase, next 5 seconds are Cross-Fade (C/F) Phase, and remaining 60 seconds are Test Phase (pure closed-loop). (C) Open-loop replay experiment. A pre-recorded refuge trajectory from the closed-loop experiment is used as refuge motion $r(t)$. (D) Sample data from an open-loop replay experiment where the same closed-loop refuge trajectory was used. Last 60 seconds are Test Phase. Fish trajectories in (B) and (D) are markedly different despite identical refuge trajectories.

In the Initation Phase, the refuge motion was a sinusoidal trajectory at 0.45 Hz, ramped over 5 s. As in previous studies [2, 4], the gradual introduction of refuge motion reduces startle responses. Visual inspection of fish motion during this phase also provides a confirmation that the animal is attending to the tracking task (in this study, no trials were rejected based on visual inspection of the Initiation Phase). Pilot experiments were conducted without this Initiation Phase, and the animals were often startled at the beginning of the Test Phase. The parameters of the Initial Phase (duration, amplitude, frequency, ramp profile) were selected based on extensive prior experience with similar studies and fall well within the locomotor tracking performance (amplitude and bandwidth) of the fish. It is possible that details of the Initial Phase may affect details of the behavior during the Test Phase, so the same Initiation Phase parameters were used across all conditions to ensure consistency.

The Cross-Fade Phase provided a smooth transition from open-loop to closed-loop control of the refuge trajectory. During this phase, the amplitude of the open-loop sinusoidal stimulus was reduced to zero over a period of 5 s while the gain of the closed-loop component of refuge was concomitantly increased to its final test value for that experiment.

In the Test Phase of closed-loop experiments, the refuge motion was completely governed by the movement of the fish, as given in Eqn. 1. The choice of gains γ and its logic are explained later in *Details of closed-loop experiment*.

In open-loop replay experiments, an entire 70 s refuge trajectory, previously recorded in a closed-loop trial, was presented to the animal. These trajectories included the refuge motion that resulted from the Initial, Cross-Fade, and Test Phases from a previously recorded trial. As in closed-loop trials, the analysis of open-loop replay trials was restricted to the final 60 s of the trial, corresponding to the Test Phase of the closed-loop experiment.

If the fish left the refuge or the real time tracking of the fish from the video feed was lost during a trial, the trial was terminated and the data collected during that trial rejected. In such cases, the trial was repeated until completed successfully. This occurred in less than 10% of the trials, so no significant selection bias corrupted our observation.

Details of initiation and cross-fade phases

To smoothly initiate each trial, the refuge was first moved in a sinusoidal trajectory (0.45 Hz) which gradually ramped up in amplitude from 0 cm to 3 cm over the first 5 s of the trial (Initiation Phase). Over the next 5 s (Cross-Fade

Phase), the refuge input smoothly transitioned from the sinusoidal trajectory to closed-loop control (Eqn. 1), in which the refuge motions were directly proportional to those of the fish by the specified gain constant, γ. Specifically, the refuge trajectory was defined by the following:

$$r(t) = \alpha(t)A(t)\sin\left(0.45 \cdot 2\pi t\right) + (1-\alpha(t))\gamma x_{\text{fish}}(t), \tag{1}$$

where

$$A(t) = \begin{cases} 0.5 - 0.5\cos\left(0.1 \cdot 2\pi t\right), & 0 \leq t < 5 \\ 1, & 5 \leq t \leq 70 \end{cases}$$

$$\alpha(t) = \begin{cases} 1, & 0 \leq t < 5 \\ 0.5 - 0.5\cos\left(0.1 \cdot 2\pi t\right), & 5 \leq t < 10 \\ 0, & 10 \leq t \leq 70. \end{cases}$$

Here, $A(t)$ specifies the smooth onset amplitude of the sinusoidal input which initiates the trial, while $\alpha(t)$ provides a "crossfade" parameter to smoothly transition from the initial sinusoidal input to closed-loop control.

Details of closed-loop experiment

Assuming constant sensory slip, $e_{\text{rms}} = E$, we have

$$x_{\text{RMS}} = \frac{1}{1-\gamma}E = \beta E \quad \text{for} \quad \gamma < 1. \tag{2}$$

Note that a gain of $\gamma = 1$ ($\beta = \infty$) leads to a singularity in the closed-loop, whereby the fish is unable to change its relative position in the tube, ultimately causing the linear actuator to hit a travel limit. Gains of greater than 1 negates the sign of reafferent feedback, making it difficult for the fish to stabilize its position inside the refuge; such conditions, while potentially interesting, are beyond the scope of the present study.

To test the robust slip hypothesis, we selected a set of 20 proportional gain constants which were hyperbolically along the real line between $\gamma = -1$ and $\gamma = +0.5$ such that values for $\beta = (1-\gamma)^{-1}$ were uniformly spaced. This choice of gain spacing makes the comparison between theoretical expectations and experimental observations visually apparent: if slip is maintained constant by the fish, then we expected x_{RMS} to be linear (with slope E) when plotted as a function of $\beta = (1-\gamma)^{-1}$.

Six individuals (N=6) were presented with closed-loop trials at each of 20 gain values. For each gain value, we performed trials with two complementary lighting conditions: 'lights-on' and 'lights-off'. This gave a set of 40 unique trial conditions. We performed 3 replicate trials for each set of conditions, resulting in a total of 120 trials per individual. To reduce the possibility of learning or sequential ordering effects, we randomized the order of all trial conditions (gain and lighting). Each trial was separated by a rest period of 2-3 minutes. For any two successive trials with the same lighting condition, the opposite lighting condition was imposed during the rest period (for example, two consecutive 'lights-on' trials would be separated by a 'lights-off' rest interval).

Details of open-loop replay experiment

A separate open-loop replay experiment (see Fig. 1 C,D) was designed to ensure that changes in behavior resulted from the coupling between the fish movement and the refuge movement, and not simply as a consequence of the refuge motion itself. Five individuals (N = 5) were presented with closed-loop trials using gain values of -1 and $+0.22$. For each gain value, the position of the refuge was recorded throughout three replicate closed-loop trials, giving three distinct refuge trajectories for playback. Each of these refuge trajectories was played back in five open-loop trials, in which the refuge motion pattern presented to the fish was the same trajectory as recorded in an earlier corresponding closed-loop trial. Additionally, five closed-loop trials were recorded for each gain value (these trials were not played back in open-loop) to offer further behavioral data for the closed-loop condition. The order of all trials was randomized for each individual, with the constraint that a closed-loop trial had to be completed (its trajectory recorded) before any of its five corresponding open-loop replay trials. This resulted in a total of 46 trials per fish (two gain values, each with three closed-loop trials recorded for playback, 15 open-loop playback trials, and five closed-loop trials for further comparison, one lighting condition: 'lights-off').

Motion analysis

For each trial ($n = 720$ for closed-loop, $n = 230$ for open-loop), the digitized position of the fish for each frame was converted from raw pixel data to length units (centimeters), giving the longitudinal position of the fish as a time-varying signal over the period of a trial. The longitudinal position of the refuge for each trial was available directly in length units from the custom code which controlled the refuge (LabView, National Instruments, Austin, TX, USA). We calculated the RMS of the mean-subtracted longitudinal position of the fish, giving a single value per trial to represent the amount of motion of the fish. Occasional whole-body bending and transverse motion were not used in our analysis, thereby treating the refuge tracking behavior as a one-dimensional task [2, 5]. From the mean-subtracted longitudinal position of the fish ($x(t)$), we calculated the velocity ($\frac{d}{dt}x(t)$), slip ($e(t) = r(t) - x(t)$), and slip-velocity ($\frac{d}{dt}e(t)$) to gain further insight regarding locomotor behavior. For the closed-loop experiment, we calculated RMS of each of these and averaged over each set of three replicate trials to characterize individual behavior across all trial conditions. For the open-loop experiment, we calculate the RMS of $x(t)$ for each trial and compared the amount of movement between closed-loop trials and the corresponding open-loop playback trials.

Analysis of open-loop replay data

For the statistical analysis of the open-loop replay experimental data we adopted the following simplification approach. For an individual, at a specific gain, we computed the ratio of RMS of each of the 5 open-loop replicates to the corresponding closed-loop data (movement/slip). We averaged these 5 ratios to get one value per closed-loop trajectory used in the open-loop replay experiment. Repeating the process for other two closed-loop trajectories we got three values and averaged these three values to get one representative value for an individual at a specific gain. Thus we ended up with total of two sets of 5 values corresponding to gain -1 and $+0.22$. The statistics reported in the main paper were performed on these datasets.

Epoch analysis

Using a custom written MATLAB (MathWorks, Natick, MA, USA) script we detected the the direction reversal points on time series active movement data. Based on this, we calculated the epoch distance (active movement between successive direction reversals) and epoch duration (time between successive direction reversals).

Estimation of active probe signal from experimental data and system parameters

The original system and the plant transfer functions are taken as described in previous studies [5, 6]. The transfer functions of task plant/swimming mechanics, $P(s)$, and overall system, $H(s)$, are given as follows (see Fig. 2 A):

$$P(s) = \frac{\kappa}{Ms^2 + Bs} \tag{3}$$

$$H(s) = \frac{\alpha\omega_n^2}{s^2 + 2\zeta\omega_n s + \omega_n^2} \tag{4}$$

$$C(s)P(s) = \frac{H(s)}{1 - H(s)} \tag{5}$$

The parameter values are listed in Table I. For the estimation of the active probe signal from the experimental data of the longitudinal position of the fish, $X(s)$ we computed the transfer function, $G_\gamma(s)$ from $A(s)$ to $X(s)$ as follows (see Fig. 2 B):

$$\begin{aligned} X(s) &= G_\gamma(s)X(s) \\ G_\gamma(s) &= \frac{P(s)}{1 + C(s)P(s)(1-\gamma)} \\ \Rightarrow G_\gamma(s) &= \frac{\kappa}{Ms^2 + Bs} \cdot \frac{s^2 + 2\zeta\omega_n s + \omega_n^2(1-\alpha)}{s^2 + 2\zeta\omega_n s + \omega_n^2(1-\alpha\gamma)} \end{aligned}$$

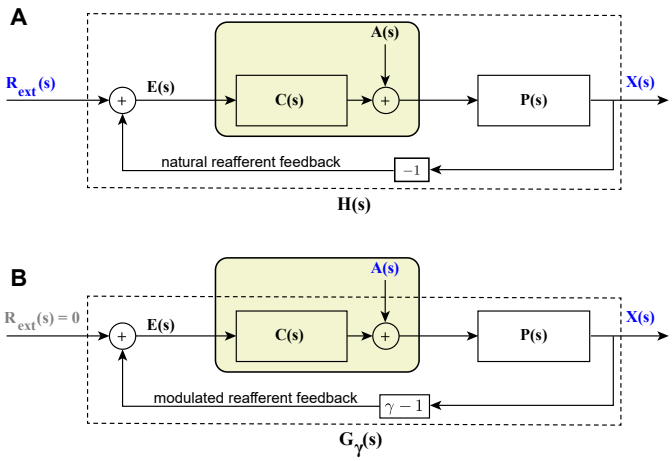

FIG. 2. Schematic of original and modified closed-loop fish system in the frequency domain. (A) Closed-loop model of tracking behavior of the fish. Blocks and arrows depict different subsystems and signals, respectively, in the frequency domain. The transfer function, $H(s)$, of the fish from external input, $R_{ext}(s)$, to output, $X(s)$, includes the task controller, $C(s)$, and the swimming mechanics/task plant, $P(s)$. The error signal, $E(s)$, representing the difference between $R_{ext}(s)$ and the reafferent feedback, is the input to the controller. $A(s)$ represents the active probe signal in the frequency domain. (B) Modified system in present study. The new transfer function of the system, $G_\gamma(s)$, from $A(s)$ to $X(s)$, is a function of the gain constant γ due to the modulation in the reafferent feedback. External input signal, $R_{ext}(s)$, which can be used for system identification analysis [5], is zero in the present study.

TABLE I. System Parameters

Parameter	Description	Value [unit]	Reference
α	DC gain	1 [s^2]	[5]
ω_n	undamped natural frequency	$2\pi \times 1.049$ [rad s^{-1}]	[5]
ζ	damping coefficient	0.56 [unitless]	[5]
M	mass constant	2.8×10^{-3} [kg]	[6]
B	damping constant	5.3×10^{-3} [kg s^{-1}]	[6]
κ	actuator gain	2.09×10^{-3} [kg s^{-2}]	[6]

In the frequency domain,

$$A(j\omega) = \frac{X(j\omega)}{G_\gamma(j\omega)}$$

$$\Rightarrow A(j\omega)A(-j\omega) = |A(j\omega)|^2 = \frac{|X(j\omega)|^2}{|G_\gamma(j\omega)|^2}$$

Under appropriate choice of window function, power spectral density (PSD) of active probe signal, PSD$\{a(t)\}$, and the longitudinal fish position, PSD$\{x(t)\}$, are related as follows:

$$\text{PSD}\{a(t)\} = \frac{\text{PSD}\{x(t)\}}{|G_\gamma(j\omega)|^2}$$

QUANTIFICATION AND STATISTICAL ANALYSIS

All the statistical analysis were performed with custom codes written in MATLAB (MathWorks, Natick, MA, USA). The statistical tests used, as indicated in this manuscript, were as follows: one way ANOVA, Mann-Whitney Wilcoxon (MWW) test, Mann-Kendall test and Spearson's rank correlation test. For all tests significance level was set to < 0.05. The experimental data are provided as the mean plus or minus the standard error of the mean ($\mu \pm \text{SEM}$).

DATA AND SOFTWARE AVAILABILITY

An archived version of the datasets and the analysis code supporting this article will be made available through the Johns Hopkins University Data Archive with the following doi:10.7281/T1/DX9DL8.

[1] Hitschfeld ÉM, Stamper SA, Vonderschen K, Fortune ES, Chacron MJ. Effects of restraint and immobilization on electrosensory behaviors of weakly electric fish. ILAR J. 2009;50(4):361–372.
[2] Roth E, Zhuang K, Stamper SA, Fortune ES, Cowan NJ. Stimulus predictability mediates a switch in locomotor smooth pursuit performance for *Eigenmannia virescens*. J Exp Biol. 2011;214(7):1170–1180.
[3] Sutton EE, Demir A, Stamper SA, Fortune ES, Cowan NJ. Dynamic modulation of visual and electrosensory gains for locomotor control. J R Soc Interface. 2016;13(118):20160057.
[4] Stamper SA, Roth E, Cowan NJ, Fortune ES. Active sensing via movement shapes spatiotemporal patterns of sensory feedback. J Exp Biol. 2012;215(9):1567–1574.
[5] Cowan NJ, Fortune ES. The critical role of locomotion mechanics in decoding sensory systems. J Neurosci. 2007;27(5):1123–1128.
[6] Sefati S, Neveln ID, Roth E, Mitchell TR, Snyder JB, MacIver MA, et al. Mutually opposing forces during locomotion can eliminate the tradeoff between maneuverability and stability. Proc Nat Acad Sci. 2013;110(47):18798–18803.

Supplemental Information

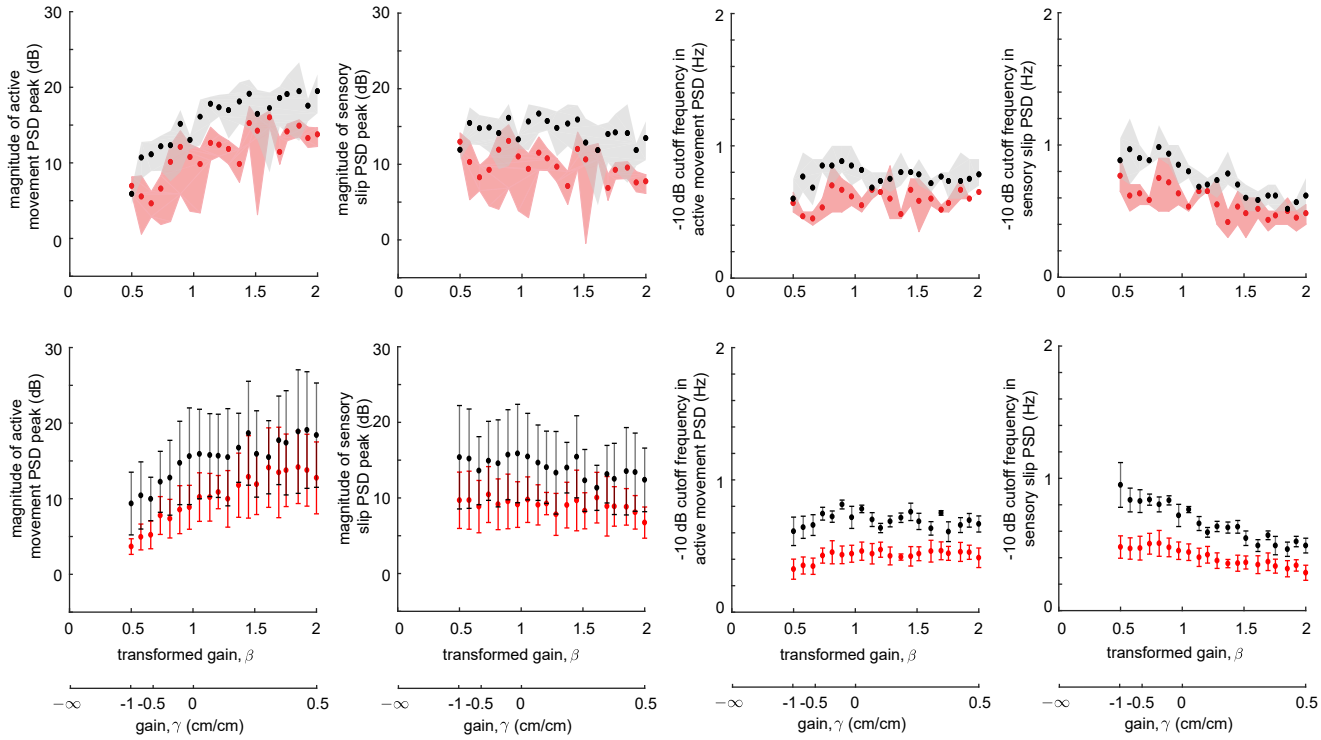

FIG. S1. Related to Figure 3. Important features of power spectral density (PSD) of active movement and sensory slip across gains. The top row presents representative data from one fish. Each marker represents respectively the peak amplitude of PSD of active movement (first column), peak amplitude of PSD of sensory slip (second column), -10 dB cut-off frequency of active movement PSD (third column) and -10 dB cut-off frequency of sensory slip PSD (fourth column) averaged across three replicates (black: 'lights-off', red: 'lights-on') at different gain values. The shaded regions denote the maximum and minimum experimental values at each gain. The bottom row represents combined data for all individuals ($N = 6$) with mean $\pm$ SEM indicated.

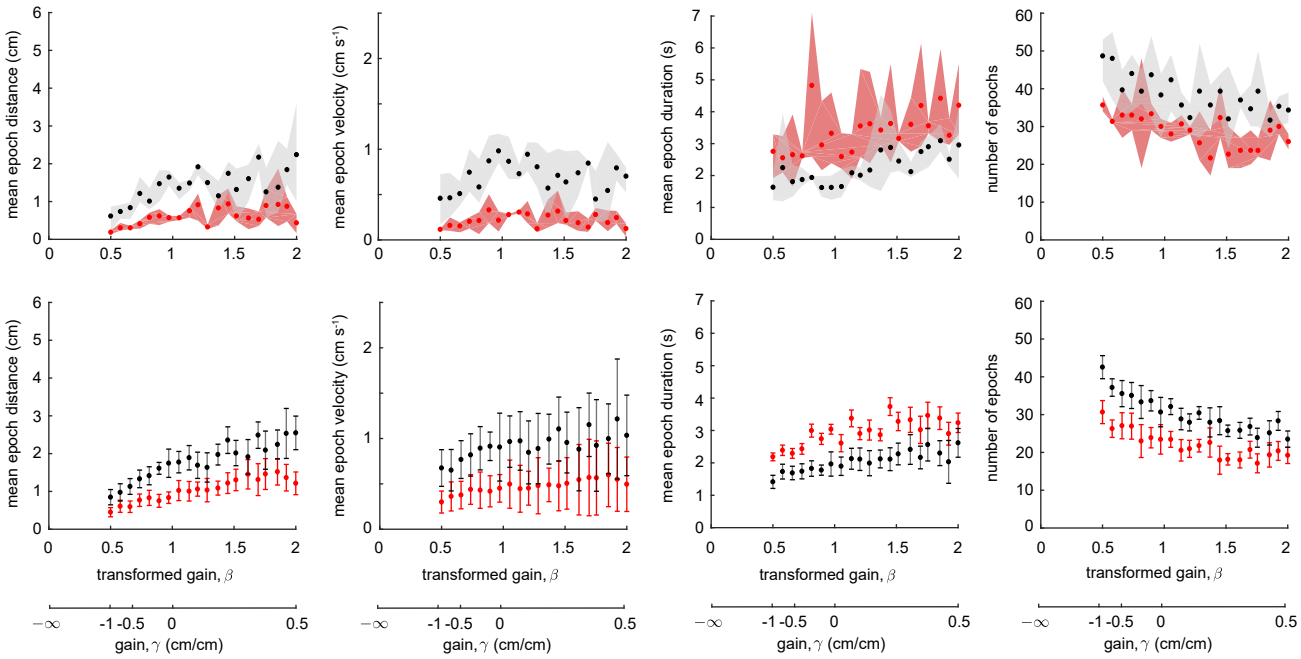

FIG. S2. Related to Figure 3. Epoch analysis. The top row presents representative data from one fish. Each marker represents respectively the mean distance traversed by the fish between consecutive direction reversals, or *epochs* (first column), the mean epoch velocity (second column), the mean duration of the epochs (third column) and the number of epochs (fourth column) averaged across three replicates (black: 'lights-off', red: 'lights-on') at different gain values. The shaded regions denote the maximum and minimum experimental values at each gain. The bottom row represents combined data for all individuals ($N = 6$) with mean $\pm$ SEM indicated. The high SEM in the combined data of mean epoch velocity does not result due to the variation among trials for an individual, rather it is caused by the variability across fish.

TABLE S1. Related to Figure 2. Adjusted R^2 values for linear, quadratic and cubic fit to the active movement data for each individual ($N = 6$) as well as to the combined data in both lighting conditions ('lights-on' and 'lights-off' trials).

R^2_{adjusted}		Fish 1	Fish 2	Fish 3	Fish 4	Fish 5	Fish 6	Combined ($N = 6$)
'lights-on'	linear fit	0.554	0.458	0.605	0.590	0.651	0.731	0.879
	quadratic fit	0.610	0.481	0.720	0.607	0.706	0.786	0.951
	cubic fit	0.595	0.450	0.705	0.587	0.695	0.774	0.949
'lights-off'	linear fit	0.215	0.266	0.627	0.610	0.462	0.040	0.649
	quadratic fit	0.592	0.322	0.826	0.620	0.681	0.508	0.878
	cubic fit	0.567	0.334	0.822	0.611	0.700	0.548	0.877

TABLE S2. Related to Figure 3. Mann-Kendall test and Sen's slope estimator for detecting increasing/decreasing trend in PSD of active movement and sensory slip. Low p value suggests existence of trend with respect to independent variable – transformed gain, β. Sen's slope estimator is a robust unbiased estimator of the true slope of the linear regressor model fitted to the data.

p-value	−10 dB cutoff frequency				Maximum amplitude			
	Active Movement		Sensory Slip		Active Movement		Sensory Slip	
	'lights-on'	'lights-off'	'lights-on'	'lights-off'	'lights-on'	'lights-off'	'lights-on'	'lights-off'
Fish 1	0.3649	0.6912	0.0458	2.65×10^{-6}	5.00×10^{-5}	3.17×10^{-4}	0.6732	0.6265
Fish 2	0.2784	0.0103	0.03	3.95×10^{-5}	3.17×10^{-4}	0.0048	0.7212	0.2561
Fish 3	0.5284	0.9463	3.49×10^{-4}	2.78×10^{-6}	5.17×10^{-4}	1.34×10^{-6}	0.556	0.2561
Fish 4	0.0628	0.0626	0.0013	4.86×10^{-5}	1.60×10^{-5}	8.32×10^{-4}	0.3468	0.381
Fish 5	0.8915	7.00×10^{-4}	4.61×10^{-5}	2.51×10^{-6}	2.85×10^{-5}	1.91×10^{-4}	0.7212	0.0297
Fish 6	0.3883	0.4915	0.0111	0.0019	4.93×10^{-7}	0.0021	0.6265	0.1441
sen's slope	−10 dB cutoff frequency				Maximum amplitude			
	Active Movement		Sensory Slip		Active Movement		Sensory Slip	
	'lights-on'	'lights-off'	'lights-on'	'lights-off'	'lights-on'	'lights-off'	'lights-on'	'lights-off'
Fish 1	0	0	−0.090	−0.449	6.127	23.028	−0.745	−1.697
Fish 2	0.058	−0.146	−0.1483	−0.378	15.191	32.228	−1.635	−13.076
Fish 3	0	0	−0.157	−0.318	14.757	56.780	−4.236	−5.548
Fish 4	0.130	0.066	−0.191	−0.210	13.269	40.367	0.932	−6.648
Fish 5	0	−0.148	−0.247	−0.488	27.781	65.039	−1.745	−14.400
Fish 6	0.017	−0.079	−0.091	−0.339	9.708	12.058	0.343	−3.821

TABLE S3. Mann-Kendall test for detecting trend in mean and maximum epoch parameters – distance, velocity and duration. Low p value suggests existence of trend with respect to independent variable – transformed gain, β.

	Mean Epoch Distance		Mean Epoch Velocity		Mean Epoch Duration		Maximum Epoch Distance		Maximum Epoch Velocity		Maximum Epoch Duration	
	'lights-on'	'lights-off'	'lights-on'	'lights-off'	'lights-on'	'lights-off'	'lights-on'	'lights-off'	'lights-on'	'lights-off'	'lights-on'	'lights-off'
Fish 1	1.78×10^{-2}	1.05×10^{-3}	0.721	0.820	3.88×10^{-3}	1.47×10^{4}	3.15×10^{-3}	2.12×10^{-2}	0.871	0.871	8.59×10^{-3}	0.012
Fish 2	5.17×10^{-4}	1.65×10^{-3}	0.163	0.206	0.209	0.564	8.59×10^{-3}	1.25×10^{-2}	0.581	0.111	0.183	0.922
Fish 3	1.2×10^{-5}	1.0×10^{-5}	3.17×10^{-4}	1.47×10^{-4}	8.59×10^{-3}	3.17×10^{-4}	9.0×10^{-6}	3.0×10^{-6}	7.44×10^{-2}	0.230	0.599	0.838
Fish 4	5.0×10^{-5}	9×10^{-5}	1.79×10^{-2}	1.13×10^{-4}	2.12×10^{-2}	0.23	2.46×10^{-4}	6.58×10^{-4}	6.44×10^{-2}	0.820	5.56×10^{-2}	0.417
Fish 5	2.1×10^{-5}	1.6×10^{-5}	2.06×10^{-3}	2.12×10^{-2}	1.32×10^{-3}	1.25×10^{-2}	0.632	0.442	0.206	7.44×10^{-2}	2.06×10^{-3}	2.97×10^{-2}
Fish 6	2.06×10^{-3}	0.256	9.47×10^{-2}	2.11×10^{-2}	4.76×10^{-3}	2.06×110^{-3}	8.6×10^{-5}	0.112	0.347	0.284	4.7×10^{-3}	2.97×10^{-2}
Combined ($N = 6$)	3.51×10^{-7}	2.49×10^{-7}	2.55×10^{-6}	1.47×10^{-4}	1.05×10^{-3}	2.55×10^{-6}	1.23×10^{-7}	1.19×10^{-5}	0.041	0.50	6.58×10^{-4}	3.88×10^{-3}

TABLE S4. Related to FIgure 4. Mann-Kendall test for detecting trend in PSD of active probe signal, $a(t)$. Low p value suggests existence of trend with respect to independent variable – transformed gain, β .

	Unity amplitude crossover frequency					
	Fish 1	Fish 2	Fish 3	Fish 4	Fish 5	Fish 6
'lights-on'	0.2476×10^{-3}	0.1149×10^{-3}	0.0074×10^{-3}	0.0057×10^{-3}	0.0136×10^{-3}	0.0698×10^{-3}
'lights-off'	0.0008×10^{-3}	0.2927×10^{-3}	0.0001×10^{-3}	0.0145×10^{-3}	0.0014×10^{-3}	0.0271×10^{-3}

Movie S1. Related to Figure 1. Showing effect of negative gain, $\gamma = -1$ on fish movement. The blue line, aqua green line and the red line correspond to camera frame of reference, position of the fish, and position of the refuge, respectively. The top panel depicts the fish movement with respect to camera frame of reference ('what we see') whereas the middle panel shows the same with respect to the refuge (refuge position stabilized to the camera). Bottom panel shows refuge and fish trajectories. Enhancing the reafferent feedback ($\times 2$) results in less active movement.

Movie S2. Related to Figure 1. Showing effect of positive gain, $\gamma = +0.22$ on fish movement. The blue line, aqua green line and the red line correspond to camera frame of reference, position of the fish, and position of the refuge, respectively. The top panel depicts the fish movement with respect to camera frame of reference ('what we see') whereas the middle panel shows the same with respect to the refuge (refuge position stabilized to the camera). Bottom panel shows refuge and fish trajectories. Suppressing the reafferent feedback ($\times 0.78$) results in more active movement.